

Synthesis of carboxamide containing tranlylcypromine analogues as LSD1 (KDM1A) inhibitors targeting acute myeloid leukemia

Maria Teresa Borrello,^[a] Hanae Benelkebir,^[a] Adam Lee,^[a] Chak Hin Tam,^[a] Manar Shafat,^[b] Stuart A. Rushworth,^[b] Kristian M. Bowles,^[b] Leon Douglas,^[c] Patrick J. Duriez,^[c] Sarah Bailey,^[c] Simon J. Crabb,^[c] Graham Packham,^[c] and A. Ganesan^{*[a]}

In memory of the late Professor Maurizio Botta 1950-2019 for his generous friendship and his many outstanding scientific contributions to medicinal chemistry.

- [a] Dr. Maria Teresa Borrello, Dr. Hanae Benelkebir, Mr. Adam Lee, Mr. Chak Hin Tam, Prof. A. Ganesan^{*}
School of Pharmacy
University of East Anglia
Norwich NR4 7TJ, United Kingdom
E-mail: a.ganesan@uea.ac.uk
- [b] Ms Manar Shafat, Dr. Stuart A. Rushworth, Prof. Kristian M. Bowles
Norwich Medical School
University of East Anglia
Norwich NR4 7TJ, United Kingdom
- [c] Mr. Leon Douglas, Dr. Patrick J. Duriez, Dr. Sarah Bailey, Prof. Simon J. Crabb, Prof. Graham Packham
Protein Core Facility and Cancer Sciences
Cancer Research UK Centre and Experimental Cancer Medicines Centre
University of Southampton
Southampton General Hospital
Southampton SO16 6YD, United Kingdom

Supporting information for this article is given via a link at the end of the document.

Abstract: Lysine-specific demethylase 1 (LSD1/KDM1A) oxidatively removes methyl groups from histone proteins and its aberrant activity has been correlated with cancers including acute myeloid leukemia (AML). We report a novel series of tranlylcypromine analogues with a carboxamide at the 4-position of the aryl ring. These compounds, such as **5a** and **5b**, had potent submicromolar IC₅₀ values for the inhibition of LSD1 as well as cell proliferation in a panel of AML cell lines. The dose-dependent increase in cellular expression levels of H3K4me2, CD86, CD11b and CD14 supported a mechanism involving LSD1 inhibition. The *t*-butyl and ethyl carbamate derivatives of these tranlylcypromines, although inactive in LSD1 inhibition, were of similar potency in cell-based assays with a more rapid onset of action. This suggests carbamates can act as metabolically labile tranlylcypromine prodrugs with superior pharmacokinetics.

Introduction

Lysine methyltransferases (KMTs) catalyse the addition of one, two or three methyl groups to the lysine side chains in proteins.^[1] The process is dynamically reversible due to lysine demethylases (KDMs) which carry out C-H oxidation of the methyl group to a carbinolamine that undergoes hydrolysis to formaldehyde and the demethylated lysine. KDM1 comprising the two lysine-specific demethylase (LSD) isoforms LSD1 and LSD2 employs FAD (flavin adenine dinucleotide) as the oxidant. In addition, the approximately twenty human isoforms of KDM2-7 are iron(II)-dependent dioxygenases also known as Jumonji C (JmjC) demethylases. Targeting the FAD or iron cofactors respectively within these two families of KDM enzymes has

emerged as a successful strategy for the design of selective inhibitors.^[2,3]

LSD1 (KDM1A) contains SWIRM (Swi3, Rsc8 and Moira) and Tower domains that modulate its incorporation into transcriptionally activating or repressive multiprotein assemblies. As part of the CoREST (REST corepressor 1) and NuRD (nucleosome remodeling and histone deacetylase) complexes, LSD1 demethylates the nucleosome at histone H3K4 residues leading to gene silencing. Meanwhile, association with androgen or estrogen receptors promotes H3K9 demethylation and gene activation. These events are linked to cell proliferation in leukemia and hormone-dependent cancers as well as the maintenance of cancer stem cells resistant to therapy.^[4] Further validation of LSD1 for epigenetic drug discovery comes from its high expression levels in other cancer types including sarcoma, neuroblastoma, bladder, gastric and lung.^[5,6]

One approach to targeting LSD1 involves the repurposing of monoamine oxidase (MAO) inhibitors that disrupt the FAD cofactor common to both enzymes.^[7,8] The approved antidepressant (±)-tranlylcypromine (**1**, Figure 1) for example, is a substrate mimic that is oxidized to radical cation **2**, followed by strain induced cyclopropyl ring opening to the reactive intermediate **3** which covalently modifies FAD. Since the cofactor is tightly bound to LSD1, with one study reporting a K_d of 180 nM,^[9] the formation of tranlylcypromine-FAD adducts effectively results in irreversible enzyme inactivation. While tranlylcypromine is consequently being reinvestigated in clinical trials as an anticancer agent, it has a modest micromolar potency against LSD1 and inhibits MAO equally. Both the LSD1 potency and selectivity are improved in second-generation analogues featuring substitution of the aryl ring or the nitrogen (or both).^[10] One series **4** with a *para*-anilide substituent was

independently reported by Mai and Takeda.^[11–16] We were interested in the ‘reverse amide’ isosteres **5** and while our studies were in progress, a Takeda patent disclosed similar structures.^[17] Nevertheless, only compound **5a** below was described and the rest of our analogues are unique to this work. In parallel, we explored a sulfonamide series **6** which we have recently published.^[18]

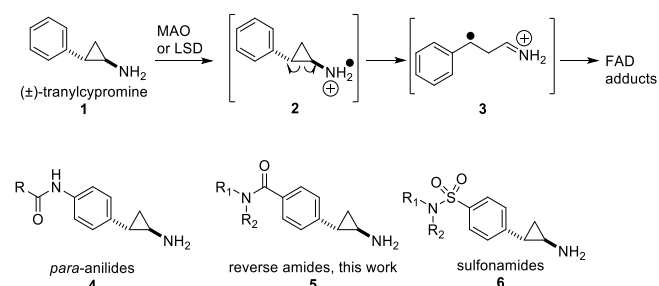
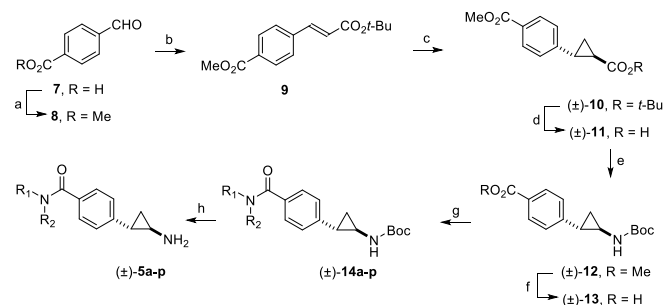


Figure 1. Mechanism of action of (±)-tranylcypromine **1** and examples of *para*-substituted second-generation analogues (±)-**4–6**.

Results and Discussion

Chemistry – analogue synthesis

Typically, the tranylcypromine scaffold is obtained from a carboxylic acid precursor which in turn arises from the [2 + 1] cyclization of arylalkenes with carbenoid or carbanion synthons. In our synthetic route, 4-formylbenzoic acid (**7**, Scheme 1) was protected as the methyl ester **8**, followed by a Horner-Wadsworth-Emmons olefination with *t*-butyl diethylphosphonoacetate to provide the differentially protected cinnamate **9**. A Johnson-Corey-Chaykovsky cyclopropanation installed the three membered ring in **10** with the *trans* configuration as confirmed by the ¹H–¹H coupling constants of the cyclopropyl moiety (*J*_{ab} = 4.2–4.5 Hz). Selective acidic removal of the *t*-butyl ester afforded the monoacid **11** which was reacted with diphenylphosphoryl azide followed by Curtius rearrangement and trapping of the resulting isocyanate with *t*-butanol to give Boc protected tranylcypromine **12**. The methyl ester was then hydrolyzed to give the common intermediate **13** which was coupled with a set of primary and secondary amines. Boc deprotection of the resulting amides **14a–p** completed the synthesis of the desired tranylcypromine analogues (±) **5a–p**.



Scheme 1. Synthesis of tranylcypromine analogues **5a–p**. a) AcCl, MeOH, 0 °C to rt, overnight, 91%; b) *t*-butyl diethylphosphonoacetate, KOt-Bu, THF, -5 °C to rt, overnight, 98%; c) Me₃S(O)I, KOt-Bu, DMSO, rt, overnight, 53%; d)

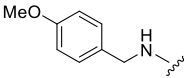
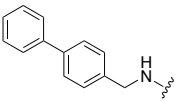
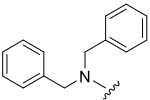
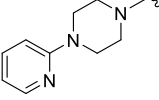
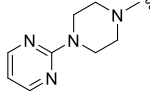
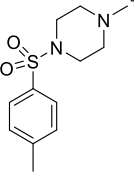
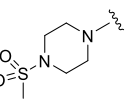
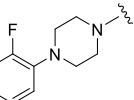
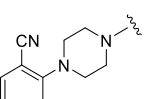
TFA, Et₃SiH, CH₂Cl₂, rt, overnight, 72%; e) diphenylphosphoryl azide, Et₃N, *t*-BuOH, reflux, 72 h, 42%; f) LiOH, aq THF, 50 °C, 2 h, 82%; g) R₁R₂NH, EDCI, HOBt, *i*-Pr₂NEt, rt, overnight, 36–67%; h) HCl, THF, 13–71%.

Biology- LSD1 inhibition and antiproliferative activity against AML cell lines

Tranylcypromine analogues **5** were investigated for their LSD1 inhibitory activity with a fluorescence-based LSD1 enzymatic assay according to our previously published procedure. Briefly, the assay uses a synthetic dimethylated histone H3K4me2 peptide as substrate and AmplexRed® detection of the H₂O₂ byproduct.^[19] While tranylcypromine itself had a IC₅₀ of 21.0 μM in this assay, the analogues were significantly more potent LSD1 inhibitors with the exception of **5h** and **5i** (Table 1). Compounds **5a–c** containing an aryl or heteroaryl substituent linked by a one or two carbon spacer to the carboxamide were submicromolar inhibitors of the enzyme. Switching to the non-aromatic cyclohexyl isosteres **5d–e** led to a loss of activity suggesting that π–π interactions might be important within the enzyme active site. In the benzyl compound **5a**, *para* substitution as in **5f–5i** led to reduced activity, most dramatically with the methoxy and biphenyl analogues. We additionally synthesized the tertiary amides **5j** with a dibenzyl group and **5k–5p** containing a 4-aminopiperazine moiety. These tertiary amides, however, did not exhibit a gain in potency compared to the simpler secondary amides.

Table 1. LSD1 enzyme inhibition by tranylcypromine analogues (±)-**5a–p**. IC₅₀ values are reported in μM ± SEM (n=3).

Compound	R ₁ R ₂ N	IC ₅₀ (μM)
5a		0.3 ± 0.08
5b		0.4 ± 0.04
5c		0.6 ± 0.08
5d		2.4 ± 0.99
5e		5.8 ± 0.47
5f		1.3 ± 0.26
5g		0.9 ± 0.18

5h		32.0 ± 0.25
5i		17.4 ± 3.9
5j		0.7 ± 0.09
5k		1.5 ± 0.2
5l		1.8 ± 0.05
5m		0.5 ± 0.01
5n		0.9 ± 0.01
5o		0.5 ± 0.04
5p		1.8 ± 0.3

Based on the enzyme assay results, selected analogues were tested for their growth inhibitory potential against acute myeloid leukemia (AML) cell lines. We selected a panel that included both the wild type MLL (mixed lineage leukemia) gene (U937, HL-60 and OCI-AML3) as well as MLL fusions arising from gene translocation (Kasumi-1: MLL-ETO; THP-1: MLL-AF9; MV4-11: MLL-AF4), since the latter are particularly sensitive to differentiation and reduced cell proliferation following LSD1 inhibition.^[20] After 72 hours incubation, tranylcypromine was found to have low antiproliferative activity, with IC₅₀ values >50 μM in five of the six cell lines tested (**Table 2**). On the other hand, the analogues with a benzylamide (**5a**, **5f**) or a phenethylamide (**5b**, **5c**) arrested proliferation of at least one cell line at submicromolar concentrations. The cellular activity generally tracked with the inhibition observed in the enzyme assay.

Table 2. Antiproliferative activity of tranylcypromine (**1**) and tranylcypromine analogues (**5**) in AML cancer cell lines. Blank cells indicate the assay was not performed with that cell line.

	Kasumi-1	U937	HL-60	OCI-AML3	THP-1	MV4-11
IC ₅₀ values in μM ± SEM (n=5)						
1	32±1.8	> 100	84±15.0	89±13.0	81±3.9	63±8.4
5a	0.3±0.01	1.6±0.4	1.7±0.4	1.8±0.8	0.1±0.1	18.1±7.2
5b	0.7±0.02	1.2±0.2	0.9±0.07	0.6±0.5	2.7±0.2	19.0±3.6
5c	0.4±0.08	0.6±0.1	6.3±0.1		1.0±0.1	1.7±0.8
5d	2.4±0.5	6.0±0.8	3.4±1.2			12.0±0.5
5e	31.0±2.7					1.0±0.2
5f	0.6±0.08				0.4±0.1	2.0±0.7
5g	2.7±0.1	34.7±3.4	>100	>100	>100	20±2.3
5l	2.3±1.4	>100	6.1±0.3	>100	>100	>100
5n	>100					2.0±0.7
5o			1.8±0.2	2.0±0.1		
5p	3.3±0.6		0.3±0.1			

Biology- mechanism of inhibition and effects on biomarkers

The nature of cellular enzyme inhibition was examined with the analogues **5a-c** through a washout experiment. Cells were exposed to the compounds for a short period of 6 hours, after which the culture medium was washed out and replaced by fresh medium without the inhibitors (**Figure 2**).

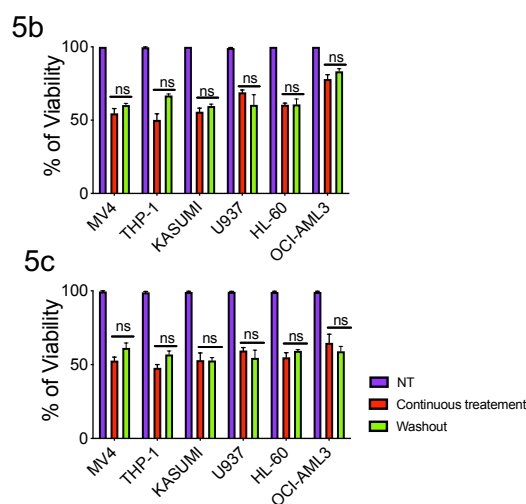


Figure 2. Washout experiment. AML cell lines were treated with 200 nM of compound **5b,c** respectively for 6 h followed by washout, or for 72 h continuously. The percentage viability was measured with Cell-Titer-Glo® and relative luminescence units (RLU) normalised to DMSO control (NT, non-treated, vehicle). Statistical analysis using two-way ANOVA and corrected for multiple comparisons using Bonferroni's test revealed non-significant (ns) variations in cells viability was found between non-treated, treated continuous and wash-out. The results are expressed as percentage of viability compared to controls. Errors bars are mean ± SEM (n=5 and three technical replicates).

To demonstrate LSD1 inhibition through cellular biomarkers, we selected **5b** as this phenethylamide compound displayed a high level of activity in the enzyme assay as well as growth inhibition of both MLL-fusion cell lines (e.g. MLL-AF4 in MV4-11 and MLL-AF9 in THP-1) and wild type MLL (e.g. HL-60). MV4-11 cells were incubated with **5b** (200 nM) for time periods of 2, 4, 6, 48 and 72 hours. After 48 and 72 hours, a time-dependent increase of H3K4me2 was observed (Figure 3), consistent with the inhibition

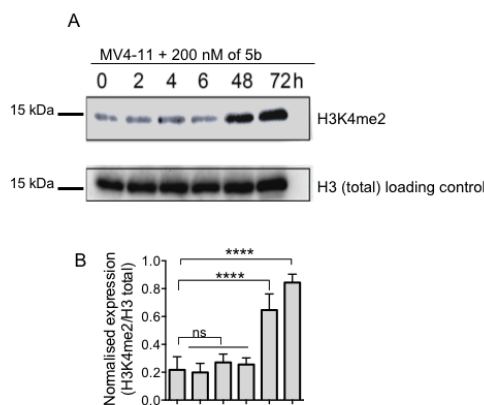


Figure 3: H3K4me2 expression upon compound 5b treatment on MV4-11 cell line. A. Immunoblot of H3K4me2 and H3 (loading control) of cell lysates prepared from MV4-11 cell line treated with compound **5b**. B. Quantification of A using ImageJ software. Mean band intensity plotted \pm SEM (n=3); One-way ANOVA was used for statistical analysis (****p<0.0001, n=3). The figure is representative of three independent biological experiments.

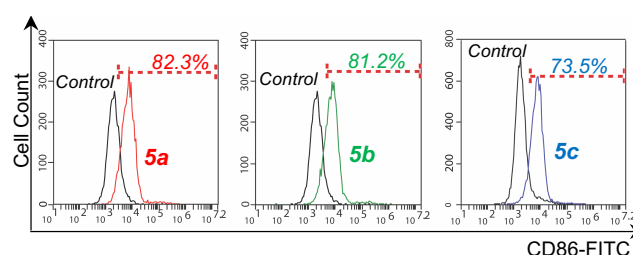


Figure 4. Evaluation of CD86 expression in MV4-11 cells upon treatment with 5a, 5b and 5c (200 nM, 48 h incubation). Cells were gated based on forward scatter (FSC) and side scatter (SSC) parameters. The X-axis indicates the mean fluorescence increase of CD86-FITC stained cells. Percentage of increase is reported compared to DMSO treated control cells. The figure is representative of three biological replicates with three technical replicates.

Further evidence for cellular LSD1 inhibition came from the increased levels of myeloid-differentiation associated cell surface proteins. CD86 (cluster of differentiation 86), a linker of the coinhibitory immune response of the CTL4 and CD86 receptor, is among the most highly upregulated genes following LSD1 inhibition and a convenient cellular biomarker.^[21] Treatment of AML cell lines with **5a**, **5b** and **5c** followed by FACS sorting analysis revealed a 70-90% increase in the expression of CD86 compared to control samples (Figure 4). In addition, we examined the levels of CD11b and CD14, two glycoproteins on the myeloid cell surface that are exclusively expressed in mature leucocytes and not in undifferentiated cells. As anticipated, **5a** and **5b** triggered cell differentiation as confirmed by a significant increase in CD11b and CD14 expression (Figure 5).

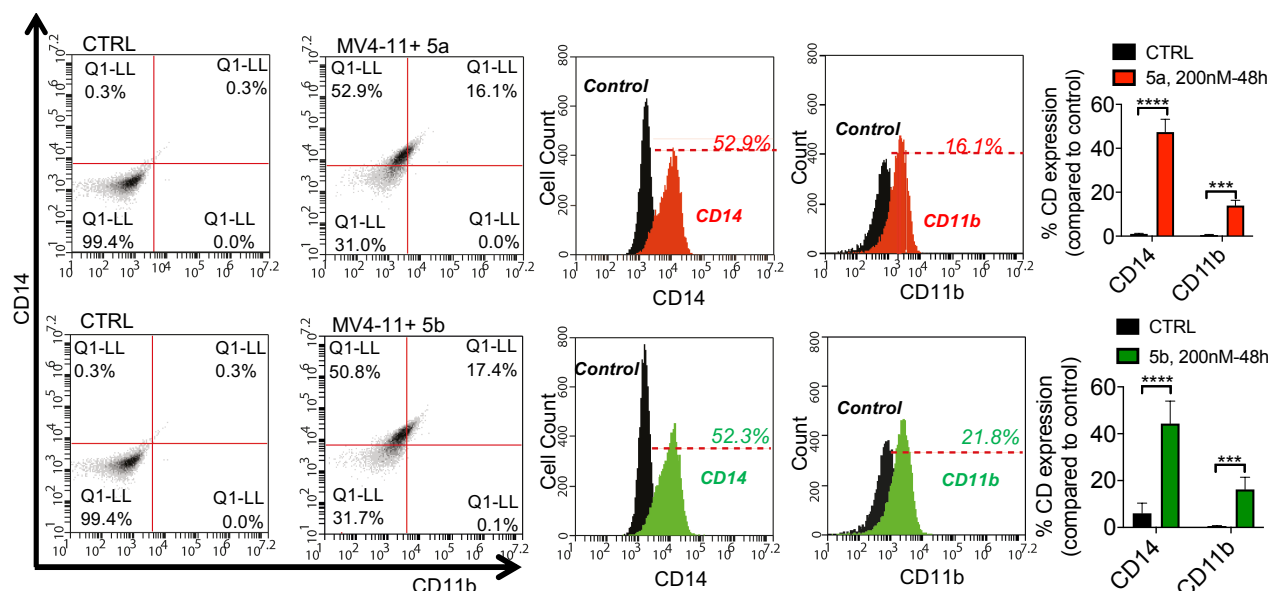


Figure 5. Effect of compounds 5a and 5b (200 nM, 48h) on the expression of CD14 and CD11b. FSC and SSC profiles were applied for the initial gating by selecting cell size and distribution and removal of cell debris. Plot A shows the isotype controls; B and C show the expression of CD11b and CD14 upon treatment with **5a** and **5b** respectively. Statistical significance was determined with two-way ANOVA and corrected for multiple comparisons with Bonferroni's test. Values are expressed as means % of CD14-CD11b increase \pm SD (n=3); ****p < 0.0001. The reported figure is representative of three independent experiments.

Biology – tranlylcypropromine versus carbamate derivatives

The mechanism of action of tranlylcypropromine (Figure 1) requires the lone pair of electrons in the amine to undergo oxidation by the FAD cofactor. As expected, the Boc protected precursors **14** of our analogues **5** were inactive in enzyme inhibition assays at the highest tested concentration of 250 μ M even at prolonged exposure times of 72 and 96 hours. However, to our surprise, the Boc carbamates displayed significant growth inhibition of the AML cell lines as illustrated for **14b** and **14c** (Figure 6), the protected versions of **5b** and **5c** respectively (Table 3 and Supplementary Figure S2-S8). Furthermore, while the tranlylcypropromines required incubation periods of 72 hours, significant reduction of cell survival was observed with the carbamates at shorter exposures of 24 and 48 hours.

Table 3. Antiproliferative activity of Boc protected tranlylcypropromines **14b,c** and **15b,c** in AML cancer cell lines. Blank cells indicate the assay was not performed with that cell line.

	Kasumi-1	U937	HL-60	OCI-AML3	THP-1	MV4-11
IC ₅₀ values in μ M \pm SEM (n=5)						
5b	0.7 \pm 0.02	1.2 \pm 0.2	0.9 \pm 0.07	0.6 \pm 0.5	2.7 \pm 0.2	19.0 \pm 3.6
14b	0.5 \pm 0.03	0.4 \pm 0.04	0.4 \pm 0.02	0.4 \pm 0.02	0.2 \pm 0.04	0.5 \pm 0.01
15b		0.3 \pm 0.03	0.5 \pm 0.08	1.4 \pm 0.5		1.3 \pm 0.3
5c	0.4 \pm 0.08	0.6 \pm 0.1	6.3 \pm 0.1		1.0 \pm 0.1	1.7 \pm 0.8
14c	0.7 \pm 0.1	0.6 \pm 0.02	0.5 \pm 0.04	0.5 \pm 0.07	0.6 \pm 0.05	0.6 \pm 0.1
15c			0.7 \pm 0.03	0.5 \pm 0.04	0.3 \pm 0.01	0.5 \pm 0.02

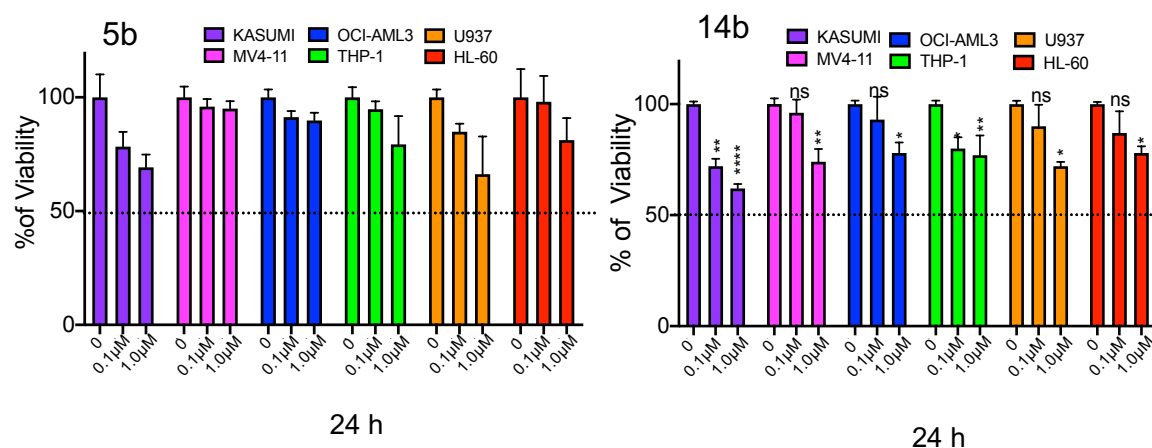


Figure 5. Viability upon 24-hour with TCP-derivative carboxamides **5b** and **14b** on AML cancer cells at 0.1 μ M and 1 μ M. Two-way ANOVA analysis corrected with Dunnet's test for multiple comparison revealed a non-significant decrease in cell viability upon 24 h compared to Non treated (NT, vehicle) upon 5b treatment and a significant decrease in cell viability after treatment with compound **14b** (* p = 0.01 ** p = 0.001 **** p < 0.0001) The results are expressed as percentage of viability compared to controls. Errors bars are mean \pm SEM (n=5 and three technical replicates).

To understand if these effects were specific to the Boc compounds, we prepared the ethyl carbamates **15b** and **15c**, which also exhibited similar levels of antiproliferative activity (Table 3 and Supplementary Figures).

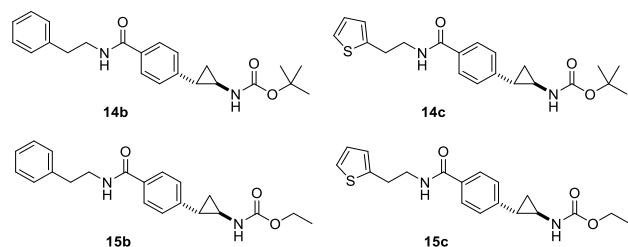


Figure 6. Structures of tranlylcypropromine carbamates **14b,c** and **15b,c**.

The carbamates were indistinguishable from the tranlylcypropromines in their cellular phenotypic effects with a dose-dependent increase in H3K4me2, CD86, CD11b and CD14 (Supplementary figures S2-S8). Some of our compounds were also tested as LSD1 inhibitors against the parasite *Schistosoma mansoni*, the causative agent of the neglected tropical disease schistosomiasis. In this context as well, the Boc tranlylcypropromines **14** were more active than the free amines **5**.^[22] Based on these results, we believe the carbamates are acting as prodrugs that undergo hydrolysis to liberate the active compound intracellularly, and we have observed a similar phenomenon in our sulfonamide series **6**.^[18] This suggests that derivatization of tranlylcypropromines is a promising avenue for the improvement of pharmacokinetic properties, as indicated by the faster time course of cancer cell line and parasite inhibition observed with the carbamates. This probably reflects more efficient cell permeability of the carbamates relative to the ionizable amine present in tranlylcypropromines.

Conclusion

We report a series of tranlycypromines containing a *para*-carboxamide substituent in the phenyl ring. Many of the compounds, including **5a** and **5b** with the relatively simple benzyl and phenethyl substituent respectively, robustly inhibit LSD1 with submicromolar IC₅₀ values and have similar levels of potency in the inhibition of AML cell lines. We demonstrated LSD1 as the cellular target through measurement of increased histone methylation and increased expression of cellular differentiation markers CD86, CD11b and CD14. Interestingly, *t*-butyl and ethyl carbamate derivatives of the tranlycypromines were potent in cellular assays although unable to inhibit LSD1 *in vitro*, suggesting they act as metabolically labile prodrugs.

Experimental Section

Chemistry. General procedures. All chemicals were purchased from Sigma Aldrich, Lancaster Synthesis GmbH, Alfa Aesar, and Novabiochem and used without further purification. TLC was used to monitor reactions and performed on aluminium-backed silica gel coated plates (Merck DC, Alufolien Kieselgel 60 F₂₅₄) with spots visualized by UV-light (λ 254 nm). Product concentration after reactions and extractions involved the use of a rotary evaporator operating at reduced pressure of ca. 20 Torr and the term *in vacuo* refers to solvent concentration at reduced pressure. When necessary products were purified by flash chromatography using silica gel (MN Kieselgel 60, 40–63 μ m, 230–400 mesh ASTM). NMR spectra were recorded on a Bruker AC 400 spectrometer and the spectra were calibrated to the residual deuterated solvent peak (CDCl₃, CD₃OD or DMSO-*d*₆). The chemical shifts are reported in δ (ppm) units followed by brackets for protons containing spectral details in this order: multiplicity (s: singlet, d: doublet, t: triplet, q: quartet, m: multiplet, br: broad), coupling constants (reported in Hz), number of protons (from integration). HRMS were acquired through the EPSRC National Mass Spectrometry Service Centre, Swansea. Melting points were determined with a STUART Melting point SMP10. IR spectra were determined with Perkin Elmer, Spectrum GX, FT-IR system. RP-HPLC analyses were performed with an Agilent Technologies 1200 series chromatograph with an Agilent Technologies ZORBAX Eclipse XDB-C18 (5 μ m, 4.6×150 mm) column. Gradient used: 95:5 water: methanol with 0.05% TFA additive to 5:95 water: methanol over 15 min returning to 95:5 water: methanol over 5 min at a flow rate of 1 mL/min. Purity was monitored at 220 nm and found to be at least 95% for all compounds that were tested in biological assays.

Methyl 4-formylbenzoate (8): 4-Formylbenzoic acid (10.0 g, 66.0 mol, 1.0 equiv.) was dissolved in anhydrous MeOH (100 mL) with cooling (-5 °C) and acetyl chloride (24.1 g, 21.2 mL, 0.33 mol, 5.0 equiv.) was added dropwise over a period of 10 min. After 30 min, the reaction mixture was warmed to rt and stirred overnight. The volatiles were removed *in vacuo* and the residue dissolved in EtOAc (70 mL), washed with 1 N NaOH, (100 mL x 3) followed by sat. NaHCO₃ (50 mL x 3), H₂O (50 mL x 3) and brine (50 mL x 3). The organic phase was dried over MgSO₄, filtered and concentrated to give **8** (9.8 g, 91%) as a crystalline white solid that was used without further purification: *R*_f=0.4, (Petroleum ether/EtOAc 3:7); mp 180 °C; IR 1716, 1684, 1428 cm⁻¹; ¹H NMR (CDCl₃) δ 3.91 (s, 3H), 7.94 (d, *J*=8.5 Hz, 2H), 8.19 (d, *J*=8.3 Hz, 2H), 10.00 (s, 1H); ¹³C NMR (CDCl₃) δ 52.6, 129.6, 130.3, 135.2, 139.3, 166.2, 191.7; HRMS (ESI) *m/z* calcd. for C₉H₉O₃ [M+H]⁺ 165.0546, found 165.0545.

(E)-Methyl 4-(3-(tert-butoxy)-3-oxoprop-1-en-1-yl) benzoate (9): To a solution of KOt-Bu (7.3 g, 64.6 mmol, 1.1 equiv.) in dry THF (100 mL), *tert*-butyl diethylphosphonoacetate (16.3 g, 15.4 mL, 64.6 mmol, 1.1 equiv.) was slowly added dropwise at -5 °C for a period of 15 min. The

mixture was stirred for 1 h while maintaining the same temperature. Aldehyde **8** (9.8 g, 58.7 mmol, 1 equiv.), dissolved in dry THF (40 mL), was then added dropwise to the mixture with vigorous stirring at -5 °C for a period of 20 min. The reaction mixture was warmed to rt and stirred overnight. After that time, the reaction mixture was poured into iced H₂O (100 mL) and extracted with EtOAc (100 mL x 5). The organic phases were combined and washed with sat. NaHCO₃ (100 mL), H₂O (100 mL) and brine (100 mL) and dried over MgSO₄. Evaporation of the solvent *in vacuo* provided **9** (14.9 g, 98%) as a white crystalline solid that was used without further purification: *R*_f=0.64 (Petroleum Ether/ EtOAc 2:8); mp 64 °C; ¹H NMR (CDCl₃) δ 1.52 (s, 9H), 3.90 (s, 3H), 6.43 (d, *J*=16.0 Hz, 1H) 7.53–7.59 (m, 3H), 8.04 (d, *J* = 8.0 Hz, 2H). ¹³C NMR (CDCl₃) δ 28.2, 52.3, 80.9, 122.6, 127.8, 130.1, 131.2, 139.0, 142.1, 165.8, 166.5; HRMS (ESI) *m/z* calcd for C₁₅H₁₉O₄ [M+H]⁺ 263.1278, found 263.1278.

(±)-trans-4-Methyl[2-(tert-butoxycarbonyl) cyclopropyl]benzoate (10): A flame dried flask was charged with potassium *tert*-butoxide (0.49 g, 4.37 mmol) and trimethylsulfonium iodide (0.92 g, 4.18 mmol). DMSO (25 mL) was then added. The mixture was stirred under a nitrogen atmosphere for 30 minutes, before the dropwise addition of alkene **9** (1.00 g, 3.81 mmol) dissolved in DMSO (15 mL) over 30 minutes. The reaction mixture was stirred at ambient temperature under a nitrogen atmosphere for 16 h. Water (50 mL) and EtOAc (50 mL) were then added and the organic layer separated. The aqueous layer was extracted a further 4 times with EtOAc (50 mL) and the combined organic extracts dried over MgSO₄ and concentrated. Purification by silica gel column chromatography gave **10** as a white solid (0.56 g, 53%). *R*_f = 0.66 (petroleum ether /EtOAc 8:2); mp 40 °C; IR 1715, 1609 cm⁻¹; ¹H NMR (CDCl₃, 400 MHz) δ : 1.26 (ddd, *J*=4.8, 6.4, 8.5 Hz, 1H), 1.46 (s, 9H), 1.57 (m, 1H), 1.88 (ddd, *J*=4.4, 5.5, 8.6 Hz, 1H), 2.4 (ddd, *J*=4.1, 5.4, 9.5 Hz, 1H), 3.9 (s, 3H), 7.1 (d, *J*=8.3 Hz, 2H), 7.9 (d, *J*=8.4 Hz, 2H); ¹³C NMR (CDCl₃, 100 MHz) δ 16.5, 24.6, 24.8, 27.1, 50.9, 79.8, 124.9, 127.6, 128.7, 145.07, 165.8, 171.0; HRMS (ESI) *m/z* calcd. for C₁₆H₂₄O₄N [M+NH₄]⁺ 294.1700, found 294.1704.

(±)-trans-[2-(4-(Methoxycarbonyl)phenyl)cyclopropanecarboxylic acid (11): Trifluoroacetic acid (19.7 g, 13.2 mL, 0.17 mol, 13 equiv.) and triethylsilane (3.86 g, 5.3 mL, 33.3 mmol, 2.5 equiv.) were added to a solution of **10** (3.7 g, 13.4 mmol) in dichloromethane (40 mL). The reaction mixture was stirred at rt and monitored by TLC. After completion, the reaction mixture was co-evaporated with acetonitrile (15 mL×3) to give **11** (2.1 g, 72%) as a white crystalline solid that was used without further purification: mp 123 °C; IR 3307, 1716, 1608, 1477 cm⁻¹; ¹H NMR (CD₃OD, 400 MHz) δ 1.43 (ddd, *J*=4.6, 6.5, 8.5 Hz, 1H), 1.60 (ddd, *J*=4.6, 5.3, 9.4 Hz, 1H), 1.92 (ddd, *J*=4.1, 5.4, 8.5 Hz, 1H), 2.51 (ddd, *J*=4.0, 6.3, 9.2 Hz, 1H), 3.90 (s, 3H), 7.25 (d, *J*=8.4 Hz, 2H), 7.93 (d, *J*=8.44 Hz, 2H); ¹³C NMR (CD₃OD, 100 MHz,) δ 17.9, 25.6, 26.9, 52.5, 127.1, 129.4, 130.7, 147.6, 168.7, 176.4; HRMS (ESI) *m/z* calcd. for C₁₂H₁₁O₄ [M-H]⁻ 219.0663, found 219.0659.

(±)-trans-4-Methyl-2-[(tert-butoxycarbonyl)amino]cyclopropyl benzoate (12): The carboxylic acid **11** (2.1 g, 9.5 mmol, 1.0 equiv.), diphenylphosphoryl azide (2.86 g, 2.27 mL, 10.5 mmol, 1.1 equiv.) and triethylamine (1.44 g, 1.98 mL, 14.3 mmol, 1.5 equiv.) were combined in *tert*-butanol (11 mL) under argon, heated at reflux and allowed to react for 72 h. After that time, the reaction mixture was cooled to rt, diluted with EtOAc (20 mL) and washed with saturated Na₂CO₃ solution (20 mL×3). The organic layer was separated and the aqueous layer further extracted with EtOAc (20 mL). The organic layers were combined (40 mL), washed with sat. NaHCO₃ (10 mL), H₂O (10 mL) and brine (10 mL) and dried over MgSO₄. Concentration *in vacuo* afforded a yellow oil which was purified by silica gel column chromatography (Hexane/EtOAc 8:2) affording **12** (1.6 g, 42%) as a white crystalline solid: *R*_f=0.57 (Hexane /EtOAc 8:2); mp 45 °C; ¹H NMR (CDCl₃, 400 MHz) δ 1.20–1.24 (m, 2H), 1.43 (s, 9H), 2.07 (td, *J*=3.1, 7.6 Hz, 1H), 2.70–2.78 (m, 1H) 3.9 (s, 3H), 7.15 (d, *J*=8.5 Hz, 2H), 7.9 (d, *J*=8.4 Hz, 2H); ¹³C NMR (CDCl₃, 100 MHz) δ 14.8, 26.3, 28.0, 28.1, 28.4, 55.3, 113.8, 127.8, 132.7, 157.9; 168.7; HRMS (ESI) *m/z* calcd. for C₁₅H₁₈N₁O₄ [M-H]⁻ 276.1241, found 276.1243.

(\pm)-*trans*-4-2-[(*tert*-Butoxycarbonyl) amino]cyclopropyl]benzoic acid (**13**): To a suspension of **12** (1.6 g, 5.7 mmol, 1 equiv.) in THF:H₂O (3:1 ratio), LiOH (0.4 g, 17.32 mmol, 3 equiv.) was added and the reaction mixture heated to 50 °C and stirred for 3 h. The reaction was monitored by TLC and after completion, the reaction mixture was diluted with water (10 mL) and acidified to pH 1-2 with sat. KHSO₄. The aqueous layer was extracted with EtOAc (20 mL×3) and the combined organic layers (60 mL) were washed with sat. NaHCO₃ (10 mL), H₂O (10 mL) and brine H₂O (10 mL) and dried over MgSO₄. Solvent concentration *in vacuo* afforded **13** (1.3 g, 82%) as a white solid that was used without further purification. IR 3314, 2873, 1681, 1453 cm⁻¹; ¹H NMR (CD₃OD, 400 MHz) δ 1.21-1.25 (m, 1H), 1.43 (s, 9H), 2.04 (td, *J*=3.9, 7.9 Hz, 1H), 2.69-2.65 (m, 1H), 7.19 (d, *J*=8.3 Hz, 2H), 7.91 (d, *J*=8.3 Hz, 2H); ¹³C NMR (CD₃OD, 100 MHz) δ 17.1, 25.8, 28.7, 35.0, 80.3, 126.9, 129.4, 130.7, 148.5, 158.9, 169.9; HRMS (ESI) *m/z* calcd. for C₁₇H₂₅NO₄ [M+H]⁺ 273.1961, found 273.1962.

General procedure for 14a-p and 5a-p: To a stirring suspension of **12** in dichloromethane, Hünig's base (2 equiv.) was added and the mixture stirred until obtaining a clear solution. Subsequently, HOBt (0.2 equiv.) and EDCI (1.5 equiv.) were added and the reaction mixture stirred for 30 min. The desired amine was added to the mixture and stirring continued at rt overnight. After that time, the reaction mixture was diluted with dichloromethane and washed with 2M HCl and 1M NaOH. The organic layers were combined, washed with sat. NaHCO₃, H₂O and brine and dried over MgSO₄. Concentration *in vacuo* afforded Boc amides **14a-p**. Acid hydrolysis to remove the Boc protecting group was carried out by stirring the carbamate in 0.5 mL of THF and 0.5 mL of 4M HCl in 1,4-dioxane at rt overnight. After completion, the reaction mixture was diluted with acetonitrile and concentrated *in vacuo* afforded to give tranlylcypromines **5a-p** as their hydrochloride salt. The salts were washed with diethyl ether and purified by preparative RP-HPLC.

tert-Butyl ((\pm)-*trans*-2-(4-Phenethylcarbamoyl)phenyl)cyclopropyl carbamate (**14b**): Yield: 63%, white solid; IR 3393, 3376, 1701, 1681, 1516 cm⁻¹; ¹H NMR (CDCl₃) δ 1.17-1.20 (m, 2H), 1.44 (s, 9H), 2.05 (td, *J*=3.0, 7.7 Hz, 1H), 2.68-2.77 (m, 1H), 2.92 (t, *J*=7.0 Hz, 2H), 6.73 (q, *J*=7.2 Hz, 2H), 4.87 (br s, 1H), 6.08 (br s, 1H), 7.13 (d, *J*=8.1 Hz, 2H), 7.21-7.24 (m, 3H), 7.39-7.34 (m, 2H), 7.58 (d, *J*=8.4 Hz, 2H); ¹³C NMR (CDCl₃) δ 16.8, 22.1, 28.5, 33.1, 35.8, 41.2, 80.8, 125.39, 125.5, 125.8, 127.6, 127.76, 131.21, 137.9, 143.6, 156.7, 166.2; HRMS *m/z* calcd for C₂₃H₂₉N₂O₃ [M+H]⁺ 381.2173, found 381.2173.

tert-Butyl ((\pm)-*trans*-2-(4-(2-Thiophenylethylcarbamoyl)phenyl)cyclopropyl carbamate (**14c**): Yield, 51%, white solid; mp 94 °C; IR 3358, 3335, 1685, 1449 cm⁻¹; ¹H NMR (CDCl₃) δ 1.61-1.19 (m, 2H), 1.43 (s, 9H), 2.02-2.05 (m, 1H), 2.68-2.76 (m, 1H), 3.06 (t, *J*= 6.4 Hz, 2H), 3.62 (q, *J*=6.4 Hz, 2H), 4.93 (br s, 1H), 6.33 (br s, 1H), 6.83-6.87 (m, 1H), 6.95 (dd, *J*=3.4, 4.9 Hz, 1H), 7.10-7.16 (m, 3H), 7.61 (d, *J*=8.3 Hz, 2H); ¹³C NMR (CDCl₃) δ 15.5, 23.9, 27.5, 28.9, 31.8, 40.12, 78.6, 122.9, 124.3, 125.3, 125.8, 125.9, 131.0, 140.2, 143.6, 155.1, 166.13; HRMS *m/z* calcd. for C₂₁H₂₇N₂O₃S [M+H]⁺ 387.1737, found 387.1737.

4-((\pm)-*trans*-2- Aminocyclopropyl)-N-benzylbenzamide hydrochloride (**5a**): Yield 71%, yellow crystalline solid; mp 200 °C; IR 3336, 3289, 3075, 1674, 1437 cm⁻¹; ¹H NMR (CD₃OD) δ 1.36-1.42 (m, 1H), 1.46-1.51 (m, 1H), 2.46 (ddd, *J*=3.3, 6.6, 9.9 Hz, 1H), 2.90-2.92, (m, 1H), 4.6 (s, 2H), 7.11-7.19 (m, 3H), 7.22-7.35 (m, 4H), 7.81 (d, *J*=8.2 Hz, 2H); ¹³C NMR (CD₃OD) δ 14.3, 22.4, 32.2, 44.4, 127.5, 128.2, 128.5, 129.7, 129.5, 134.1, 140.2, 143.9, 169.6; HRMS (ESI) *m/z* calcd. for C₁₇H₁₉N₂O₁ [M+H]⁺ 267.1492, found 267.1495.

4-(\pm)-*trans* -2-Aminocyclopropyl)-N-phenethylbenzamide hydrochloride (**5b**): Yield 67%, yellow solid; mp 180 °C; IR 3283, 1637, 1545 cm⁻¹; ¹H NMR (CD₃OD) δ 1.36-1.42 (m, 1H), 1.48 (ddd, *J*=4.2, 6.7, 10.3 Hz, 1H), 2.42 (ddd, *J*=3.5, 6.3 Hz, 10.3 Hz, 1H), 2.90 (t, *J*=7.7 Hz, 3H), 3.58 (t, *J*=7.2 Hz, 2H), 7.17-7.20 (m, 1H), 7.24-7.29 (m, 6H) 7.72 (d, *J*=7.7 Hz, 2H); ¹³C NMR (CD₃OD) δ 14.3, 22.4, 32.3, 36.3, 42.6, 127.3, 127.4, 128.6,

129.5, 129.9, 134.3, 140.6, 143.8, 169.7; HRMS (ESI) *m/z* calcd. for C₁₈H₂₁N₂O [M+H]⁺ 281.1648, found 281.1648.

4-(\pm)-*trans* -2-Aminocyclopropyl)-N-(2-(thiophen-2-yl)ethyl)benzamide hydrochloride (**5c**): Yield 47%, yellow solid; mp 218 °C; IR 3318, 2775, 2977, 1626, 1505 cm⁻¹; ¹H NMR (CD₃OD) δ 1.37-1.42 (m, 1H), 1.48 (ddd, *J*=4.56, 6.7, 10.2 Hz, 1H), 2.43 (ddd, *J*=3.6, 6.0, 9.0 Hz, 1H), 2.90-2.94 (m, 1H), 3.13 (t, *J*=7.0 Hz, 2H), 3.61 (t, *J*=7.0 Hz, 2H), 6.88 (dd, *J*=1.0, 3.4 Hz, 1H), 6.91-6.94 (m, 1H) 7.20 (dd, *J*=1.0, 4.8 Hz, 1H), 7.25 (d, *J*=8.4 Hz, 2H), 7.75 (d, *J*=8.4 Hz, 2H); ¹³C NMR (CD₃OD) δ 14.3, 22.4, 30.1, 32.2, 42.7, 124.7, 126.3, 127.4, 127.8, 128.6, 134.1, 142.5, 143.7, 169.7.

4-(\pm)-*trans*-2-Aminocyclopropyl)-N-(cyclohexylmethyl)benzamide hydrochloride (**5d**): Yield 58%, yellow solid; mp 198 °C; IR 3335, 1712, 1696, 1459 cm⁻¹; ¹H NMR (CD₃OD, 400 MHz), δ 0.94-1.03 (m, 2H), 1.18-1.31 (m, 4H), 1.33-1.44 (m, 1H), 1.48-1.52 (m, 1H), 1.58-1.69 (m, 2H), 1.71-1.82 (m, 3H), 2.41-2.49 (m, 1H), 2.88-2.92 (m, 1H) 3.20 (d, *J*=6.9 Hz, 2H), 7.26 (d, *J*=8.2 Hz, 2H), 7.76 (d, *J*=8.2 Hz, 2H); ¹³C NMR (CD₃OD, 100 MHz) δ 14.3, 22.4, 26.9, 27.6, 32.3, 39.2, 39.4, 47.2, 127.4, 128.6, 134.3, 143.6, 169.8; HRMS (ESI) *m/z* calcd. for C₁₇H₂₅N₂O [M+H]⁺, 273.1961, found 273.1962.

4-(\pm)-*trans*-2-Aminocyclopropyl)-N-(2-cyclohexylethyl)benzamide hydrochloride (**5e**): Yield 33%, yellow solid; mp 79 °C; IR 3318, 1632, 1539, 1449 cm⁻¹; ¹H NMR (DMSO-*d*₆, 400 MHz) δ 0.84-0.96 (m, 2H), 1.08-1.31 (m, 5H), 1.36-1.44 (m, 2H), 1.45-1.51 (m, 1H), 1.64-1.80 (m, 5H), 2.43 (ddd, *J*=3.5, 5.5, 10.1 Hz, 1H), 2.81-2.89 (m, 1H), 3.22-3.29 (m, 2H), 7.25 (d, *J*=8.3 Hz, 2H), 7.75 (d, *J*=8.3 Hz, 2H), 8.39 (t, *J*=6.0 Hz, 1H), 8.64 (br s, 2H); ¹³C NMR (CD₃OD, 100 MHz) δ 14.3, 22.4, 27.4, 27.6, 32.2, 34.3, 36.8, 37.9, 38.8, 127.4, 128.6, 134.3, 143.6, 169.6; HRMS (ESI) *m/z* calcd. for C₁₈H₂₇N₂O [M+H]⁺ 287.2118, found 287.2119.

4-(\pm)-*trans*-2-Aminocyclopropyl)-N-(4-fluorobenzyl)benzamide hydrochloride (**5f**): Yield 45%, yellow solid; mp 98 °C; IR 335, 2486, 1620, 1516, 1458 cm⁻¹; ¹H NMR (CD₃OD, 400 MHz) δ 1.37-1.42 (m, 1H), 1.49 (ddd, *J*=4.7, 7.0, 10.2 Hz, 1H), 2.43 (ddd, *J*=3.6, 6.5, 10.0 Hz, 1H), 2.89-2.96 (m, 1H), 4.53, (s, 2H), 7.0 (t, *J*=8.7 Hz, 2H), 7.26 (d, *J*=8.2 Hz, 2H), 7.36 (m, 2H), 7.81 (d, *J*=8.3 Hz, 2H); ¹³C NMR (CD₃OD, 100 MHz) δ 14.3, 22.4, 32.3, 43.8, 116.2, 127.5, 128.5, 130.4, 133.9, 136.3, 143.9, 163.5 (d, *J*_{F-C}=220 Hz), 169.6; HRMS (ESI) *m/z* calcd. for C₁₇H₁₈F₁N₂O [M+H]⁺ 285.1398, found 285.1402.

4-(\pm)-*trans* -2-Aminocyclopropyl)-N-(4-bromobenzyl)benzamide hydrochloride (**5g**): Yield 65 %, white solid; mp 97 °C; IR 3320, 3035, 2665, 1637, 1533, 14893 cm⁻¹; ¹H NMR (CD₃OD, 400 MHz) δ 1.37-1.42 (m, 1H), 1.46-1.51 (m, 1H), 2.44 (ddd, *J*=3.2, 6.3, 9.7 Hz, 1H), 2.90-2.93 (m, 1H), 4.52 (s, 2H), 7.26 (d, *J*=8.0 Hz, 4H), 7.47 (d, *J*=8.3 Hz, 2H), 7.83 (d, *J*=8.3 Hz, 2H); ¹³C NMR (CD₃OD, 100 MHz) δ 14.4, 22.4, 32.3, 43.9, 121.8, 127.5, 128.8, 130.5, 132.6, 133.9, 139.6, 144.00, 169.7; HRMS (ESI) *m/z* calcd. for C₁₇H₁₈BrN₂O [M+H]⁺ 345.0597, found 345.0602.

4-(\pm)-*trans*-2-Aminocyclopropyl)-N-(4-methoxybenzyl)benzamide hydrochloride (**5h**): Yield 52%, yellow solid; mp 123 °C; IR 3364, 1672, 1528 cm⁻¹; ¹H NMR (CD₃OD, 400 MHz) δ 1.36-1.41 (m, 1H), 1.49 (ddd, *J*=4.6, 6.7, 10.5 Hz, 1H), 2.44 (ddd, *J*=3.4, 6.3, 9.8 Hz, 1H), 2.91, (ddd, *J*=4.0, 7.9, 11.7 Hz, 1H), 3.76 (s, 3H), 4.48 (s, 2H), 6.87 (d, *J*=8.6 Hz, 2H), 7.25 (d, *J*=8.4 Hz, 2H), 7.26 (d, *J*=8.4 Hz, 2H), 7.79 (d, *J*=8.1 Hz, 2H); ¹³C NMR (CD₃OD, 100 MHz) δ 14.3, 22.4, 32.3, 43.9, 55.7, 114.9, 127.5, 128.7, 129.8, 132.2, 134.1, 143.9, 160.4, 169.5; HRMS (ESI) *m/z* calcd. for C₁₈H₂₁N₂O₂ [M+H]⁺ 297.1598, found 297.1595.

N-([1,1'-Biphenyl]-4-ylmethyl)-4- (\pm *trans* -2 -aminocyclopropyl) benzamide hydrochloride (**5i**): Yield 34%, yellow solid; IR 3402, 3045, 1715, 1632, 1540 cm⁻¹; ¹H NMR (CD₃OD, 400 MHz) δ 1.38-1.43 (m, 1H), 1.46-1.50 (m, 1H), 2.43 (ddd, *J*=3.5, 6.3, 10.2 Hz, 1H), 2.92 (ddd, *J*=3.7, 7.9, 11.6 Hz, 1H), 4.61 (s, 2H), 7.26-7.29 (m, 2H), 7.30-7.34 (m, 1H), 7.39-7.45 (m, 4H), 7.56-7.60 (m, 4H), 7.83 (d, *J*=8.4 Hz, 2H); ¹³C NMR

(CD₃OD, 100 MHz) δ 14.3, 22.4, 32.2, 44.1, 127.4, 127.8, 128.0, 128.2, 128.7, 128.9, 129.7, 134.0, 139.2, 141.3, 142.0, 143.8, 169.6.

4-(\pm)-trans-2-Aminocyclopropyl)-N,N-dibenzylbenzamide hydrochloride (5j): Yield 52%, yellow solid; IR 3214, 1645.7, 1620, 1452 cm⁻¹; ¹H NMR (CD₃OD, 400 MHz) δ 1.37-1.38 (m, 1H), 1.49-1.56 (m, 1H), 2.43 (ddd, *J*=3.2, 6.4, 9.8 Hz, 1H), 2.96-2.90 (m, 1H), 4.43 (br s, 2H), 4.66 (br s, 2H), 7.12 (br s, 2H), 7.24-7.30 (m, 7H), 7.32-7.39 (m, 5H), 7.43-7.50 (m, 2H); ¹³C NMR (CD₃OD, 100 MHz) δ 14.1, 22.3, 32.3, 53.7, 127.6, 128.0, 128.2, 128.7, 129.8, 129.9, 135.5, 142.2, 174.2; HRMS (ESI) *m/z* calcd. for C₂₄H₂₅N₂O₁ [M+H]⁺, 357.1961, found 357.1960.

4-(\pm)-trans-2-Aminocyclopropyl)-phenyl)-4-(pyridin-2-yl)piperazin-1-yl)methanone hydrochloride (5k): Yield 13%, orange oil; IR 3358, 1603, 1545, 1435 cm⁻¹; ¹H NMR (CD₃OD, 400 MHz) δ 1.37-1.43 (m, 1H), 1.51 (ddd, *J*=4.4, 6.6, 11.1 Hz, 1H), 2.48 (ddd, *J*=3.5, 6.3, 10.0 Hz, 1H), 2.93 (ddd, *J*=4.4, 7.6, 11.2 Hz, 1H), 3.8 (br s, 8H), 7.06 (t, *J*=6.5 Hz, 1H), 7.32 (d, *J*=8.0 Hz, 2H), 7.42 (d, *J*=9.2 Hz, 1H), 7.48 (d, *J*=8.0 Hz, 2H), 8.0 (dd, *J*=1.24, 7.9 Hz, 1H), 8.05 (dt, *J*=1.6, 8.5 Hz, 1H); ¹³C NMR (CD₃OD, 100 MHz) δ 14.3, 22.4, 32.2, 44.8, 47.2, 114.3, 127.8, 128.8, 131.1, 134.5, 137.5, 142.8, 145.7, 153.7, 172.6; HRMS (ESI) *m/z* calcd. for C₁₉H₂₃N₄O [M+H]⁺ 323.1866, found 323.1869.

4-(\pm)-trans-2-Aminocyclopropyl)-phenyl)-(4-(pyrimidin-2-yl)piperazin-1-yl)methanone hydrochloride (5l): Yield 22 %, red oil; IR 3353, 1678, 1632, 1551 cm⁻¹; ¹H NMR (CD₃OD, 400 MHz) δ 1.39-1.45 (m, 1H), 1.47 (ddd, *J*=4.5, 6.9, 10.1 Hz, 1H), 2.44 (ddd, *J*=3.6, 6.4, 10.2 Hz, 1H), 2.92-2.96 (m, 1H), 3.53 (br s, 2H), 3.82 (br s, 4H), 3.94 (br s, 2H), 6.66 (t, *J*=4.7 Hz, 1H), 7.29 (d, *J*=8.2 Hz, 2H), 7.42 (d, *J*=8.3 Hz, 2H), 8.35 (d, *J*=4.8 Hz, 2H); ¹³C NMR (CD₃OD, 100 MHz) δ 14.2, 22.4, 32.1, 40.4, 41.7, 111.8, 127.7, 128.6, 135.2, 142.3, 159.1, 162.8, 172.45; HRMS (ESI) *m/z* calcd. for C₁₈H₂₂N₅O [M+H]⁺ 324.1819, found 324.1824.

4-(\pm)-trans-2-Aminocyclopropyl)-phenyl)-(4-(phenylsulfonyl)piperazin-1-yl)methanone hydrochloride (5m): Yield 25%, white solid; IR 3392, 1637, 1652, 1551 cm⁻¹; ¹H NMR (CD₃OD, 400 MHz) δ 1.33-1.38 (m, 1H), 1.45-1.50 (m, 1H), 2.41-2.43 (m, 1H), 2.45 (s, 3H), 2.87-2.89 (m, 1H), 3.00 (br s, 4H), 3.56 (br s, 2H), 3.77 (br s, 2H), 7.22 (d, *J*=7.6 Hz, 2H), 7.30 (d, *J*=7.6 Hz, 2H), 7.44 (d, *J*=7.8 Hz, 2H), 7.65 (d, *J*=7.9 Hz, 2H); ¹³C NMR (CD₃OD, 200 MHz) δ 14.2, 21.5, 22.3, 32.2, 44.2, 47.2, 127.7, 128.6, 128.9, 130.9, 133.8, 134.5, 142.4, 145.6, 172.2; HRMS (ESI) *m/z* calcd. for C₂₁H₂₆N₃O₃S [M+H]⁺ 400.1689, found 400.1687.

4-(\pm)-trans-2-Aminocyclopropyl)-phenyl)-(4-(methylsulfonyl)piperazin-1-yl)methanone hydrochloride (5n): Yield 37%, white solid; IR 3387, 1614, 1562 cm⁻¹; ¹H NMR (CD₃OD, 400 MHz) δ 1.37-1.42 (m, 1H), 1.47 (ddd, *J*=4.5, 6.8, 10.3 Hz, 1H), 2.42 (ddd, *J*=3.6, 6.6, 10.2 Hz, 1H), 2.87 (s, 3H), 2.89-2.93 (m, 1H), 3.26 (br s, 4H), 3.57 (br s, 2H), 3.8, (br s, 2H), 7.28 (d, *J*=8.2 Hz, 2H), 7.41 (d, *J*=8.3 Hz, 2H); ¹³C NMR (CD₃OD, 100 MHz) δ 14.2, 22.4, 32.0, 34.8, 46.7, 68.0, 127.8, 128.6, 134.7, 142.4, 172.3; HRMS (ESI) *m/z* calcd for C₁₅H₂₄N₃O₃S [M+H]⁺ 324.1380, found 324.1380.

4-(\pm)-trans-2-Aminocyclopropyl)-phenyl)-4-(2-fluorophenyl)piperazin-1-yl)methanone hydrochloride (5o): Yield 44%, yellow solid; IR 3387, 1603, 1505, 1470 cm⁻¹; ¹H NMR (CD₃OD, 400 MHz) δ 1.37-1.42 (m, 1H), 1.44 - 1.49 (m, 1H), 2.42 (ddd, *J*=3.2, 6.3, 9.7 Hz, 1H), 2.89-2.93 (m, 1H), 3.16 (br s, 4H), 3.66 (br s, 2H), 3.94 (br s, 2H), 7.03-7.13 (m, 4H), 7.28 (d, *J*=7.6 Hz, 2H), 7.42 (d, *J*=7.8 Hz, 2H); ¹³C NMR (CD₃OD, 100 MHz) δ 14.5, 22.4, 32.4, 54.9, 68.0, 117.7, 122.3, 126.6, 127.9, 128.4, 128.9, 134.3, 135.9, 142.6, 156.6 (d, *J*_{F-C}=245.8 Hz), 172.19; HRMS (ESI) *m/z* calcd. for C₂₀H₂₃F₁N₃O [M+H]⁺ 340.1820, found 340.1821.

2-(4-(\pm)-trans-2-Aminocyclopropyl)-benzoyl)piperazin-1-yl)benzonitrile hydrochloride (5p): Yield 39%, white solid; IR 3353, 2856, 2221, 1632, 1562 cm⁻¹; ¹H NMR (CD₃OD, 400 MHz) δ 1.38-1.42 (m, 1H), 1.44-1.51 (m, 1H), 2.40-2.45 (m, 1H), 2.92 (ddd, *J*=4.2, 8.0, 11.0 Hz, 1H), 3.18 (br s, 2H), 3.56-3.59 (m, 1H), 3.64-3.68 (m, 3H), 3.71-3.74 (m, 2H), 3.95 (br s,

1H), 7.14 (t, *J*=7.4 Hz, 1H), 7.19 (d, *J*=8.2 Hz, 1H), 7.29 (d, *J*=8.0 Hz, 2H), 7.43 (d, *J*=8.0 Hz, 2H), 7.57-7.61 (m, 1H), 7.65 (dd, *J*=2.07, 9.06 Hz, 1H); ¹³C NMR (CD₃OD, 100 MHz) δ 14.2, 22.4, 32.2, 43.7, 62.2, 107.7, 119.1, 120.6, 124.0, 127.7, 128.7, 135.1, 135.3, 135.4, 142.3, 156.6, 172.3; HRMS (ESI) *m/z* calcd. for C₂₁H₂₃N₄O [M+H]⁺, 347.1866, found 347.1869.

General procedure for 15b and 15c: These carbamates were prepared from **11** by carrying out the Curtius rearrangement in the presence of ethanol to give the ethyl carbamate. The methyl ester was then deprotected and the acid coupled with 2-phenethylamine or 2-thiophenethylamine to give **15b** and **15c** respectively.

Ethyl ((\pm)-trans-2-(4-Phenethylcarbamoyl)phenyl)cyclopropyl carbamate (15b): Yield 54%, white solid; IR 3312, 3191, 1689, 1637, 1545, 1510 cm⁻¹; ¹H NMR (CDCl₃) δ 1.20-1.27 (m, 5H), 2.07-2.11 (m, 1H), 2.72-2.76 (m, 1H), 2.92 (t, *J*=6.9 Hz, 2H), 3.69 (q, *J*=6.9 Hz, 2H), 4.12 (q, *J*=6.9 Hz, 2H), 7.14 (d, *J*=7.9 Hz, 2H), 7.19-7.24 (m, 3H), 7.28-7.34 (m, 2H), 7.58 (d, *J*=7.8 Hz, 2H); ¹³C NMR (CDCl₃) δ 14.6, 16.4, 25.2, 33.1, 35.7, 41.1, 61.0, 126.6, 126.7, 126.9, 128.7, 128.8, 132.4, 138.8, 144.4, 157.1, 167.2; HRMS *m/z* calcd. for C₂₁H₂₅N₂O₃ [M + H]⁺ 353.1860, found 353.1860.

Ethyl ((\pm)-trans-2-(4-(2-Thiophenethylcarbamoyl)phenyl)cyclopropyl carbamate (15c): Yield 49%, white solid; IR 3318, 3214, 1689, 1655, 1551, 1510 cm⁻¹; ¹H NMR (CDCl₃) δ 1.20-1.23 (m, 5H), 2.06-2.10 (m, 1H), 2.70-2.74 (m, 1H), 3.13 (t, *J*=6.5 Hz, 2H), 3.69 (q, *J*=7.04 Hz, 2H), 4.11 (q, *J*=6.5 Hz, 2H), 6.85 (dd, *J*=0.9, 3.3 Hz, 1H), 6.94 (dd, *J*=3.4, 5.1 Hz, 1H), 7.13-7.17 (m, 3H), 7.61 (d, *J*=8.1 Hz, 2H); ¹³C NMR (CDCl₃) δ 14.6, 16.4, 25.2, 29.9, 33.1, 41.3, 61.0, 124.1, 125.5, 126.6, 127.0, 127.1, 132.3, 141.3, 141.5, 157.1, 167.2; HRMS *m/z* calcd. C₁₉H₂₃N₂O₃S [M+H]⁺ 359.1424, found 359.1425.

Biology.

LSD1 enzyme assay: LSD1 residual activity after incubation with the carboxamide TCP-derivatives was measured according to our previously reported assay.^[19]

AML cell line viability assay: To measure the *in vitro* compound activity, 100 μ L of cell suspension was plated out at a density of 2.5 \times 10⁴ cells/mL in 96 well plates. Tested compounds (stock 250 mM) were dissolved to the appropriate concentration in RPMI complete medium (10 \times final concentration) and 10 μ L of each concentration was immediately added to the plated cell suspension. Each concentration was assessed five times. After treatment, cells were further cultured for the reported amount of time. Cell viability was measured with CellTiter-Glo® (Promega, Southampton, UK) by adding 100 μ L of the reagent to each well. After 10 min of incubation at RT, 100 μ L of cell suspension + reagent were transferred into a white GREINER 96 well plate to eliminate straight light and bioluminescence was recorded in a BMG Cell star microplate reader. Collected raw data were normalised to control (vehicle control) and IC₅₀'s and statistical significance were determined with GraphPad Prism software (San Diego, CA).

Washout experiment: In a 96 well plate, 100 μ L suspension of the cell lines THP-1, HL-60, MV4-11, KASUMI, OCI-AML3, U937 were plated at a density of 5 \times 10⁴ cells/mL and treated with 10 μ L of LSD1 inhibitors (200 nM final concentration) or left untreated and allowed to grow for 6 h. Inhibitor-containing media was then removed by centrifugation and replaced by fresh media. Cells were further cultured for 72 h, following which cell viability was measured with CellTiter-Glo®. The viability values obtained in the washout experiment were normalised to pre-treatment levels (vehicle control). Statistical significance was determined with one-way ANOVA and corrected for multiple comparisons using Dunnett's test between the two analysed populations (continuous vs. pulsed treatment).

H3K4me2 western blotting: MV4-11 cells were plated in a 24-well plate at a seeding density of 25 \times 10⁵ cells/well. Compound **5b** was added to

the medium at a final concentration of 200 nM. Cells were cultured for 2, 4, 6, 48 and 72 h. At the end of each timepoint, cells were pelleted, washed with ice-cold PBS and lysed in RIPA lysis buffer (50 mM Tris-Cl, pH 8.0, 150 mM NaCl, 0.1% SDS, 1% Triton X-100 and 0.5% sodium deoxycholate). Lysates were cleared by centrifugation at 16,000 rpm for 20 min at 4 °C and protein concentration determined using BCA assay kit (Thermo Scientific Pierce). Samples containing 40 µg of protein were separated by electrophoresis using a sodium dodecyl sulfate-polyacrylamide gel (SDS-PAGE) on a mini (8.6×6.7 cm) format SDS-PAGE gel (BIORAD). Proteins were next transferred to a nitrocellulose membrane with 0.2 µm pore size. Blotting membranes were probed for anti-H3K4me2 (Cell signaling anti-H3K4me2 #9725) and total H3 (Abcam anti-H3 #ab100938). After incubation with secondary antibody (Goat anti-Rabbit IgG (HRP) #ab97080), detection was carried out with chemoluminescent substrate (Western Pico Super ECL reagent, Pierce) and the bands of interest visualised on an ImageQuant™ LAS 4000 Image Analyser (GE Healthcare).

Flow cytometry: Flow cytometry experiments were performed in a BD Accuri™ C6 Flow Cytometer and data analysed using BD Accuri™ C6 Software version 1.0.264.15. Antibodies for CD86, CD14, CD11b or Isotype controls were purchased from Myltenyi Biotec. Detailed protocols are reported in the SI.

Keywords: enzyme inhibitors • FAD-dependent enzymes • epigenetics • histone demethylases • acute myeloid leukemia

- [1] M. Luo, *Chem. Rev.* **2018**, *118*, 6656–6705.
- [2] T. E. McAllister, K. S. England, R. J. Hopkinson, P. E. Brennan, A. Kawamura, C. J. Schofield, *J. Med. Chem.* **2016**, *59*, 1308–1329.
- [3] A. Ganesan, *Philos. Trans. R. Soc. B Biol. Sci.* **2018**, *373*, 20170069.
- [4] P. Karakaidos, J. Verigos, A. Magklara, *Cancers (Basel)*. **2019**, *11*, 1821.
- [5] G. Verde, J. Querol-Pañós, J. Cebrià-Costa, L. Pascual-Reguant, G. Serra-Bardenys, A. Iturbide, S. Peiró, *Epigenomes* **2017**, *1*, 4.
- [6] S. Arifuzzaman, M. R. Khatun, R. Khatun, *Biomed. Pharmacother.* **2020**, *129*, 110392.
- [7] A. Lee, M. T. Borrello, A. Ganesan, in *Epigenetic Drug Discovery* (Eds.: W. Sippl, M. Jung), Wiley-VCH: Weinheim, **2019**, pp. 221-261.
- [8] S. Mehndiratta, J.-P. Liou, *RSC Med. Chem.* **2020**, DOI 10.1039/d0md00141d.
- [9] Y. C. Zheng, Y. C. Duan, J. L. Ma, R. M. Xu, X. Zi, W. L. Lv, M. M. Wang, X. W. Ye, S. Zhu, D. Mobley, et al., *J. Med. Chem.* **2013**, *56*, 8543–8560.
- [10] Y. C. Zheng, B. Yu, G. Z. Jiang, X. J. Feng, P. X. He, X. Y. Chu, W. Zhao, H. M. Liu, *Curr. Top. Med. Chem.* **2016**, *16*, 2179–2188.
- [11] C. Binda, S. Valente, M. Romanenghi, S. Pilotto, R. Cirilli, A. Karytinis, G. Ciossani, O. A. Botrugno, F. Forneris, M. Tardugno, *J. Am. Chem. Soc.* **2010**, *132*, 6827–6833.
- [12] V. Rodriguez, S. Valente, S. Rovida, D. Rotili, G. Stazi, A. Lucidi, G. Ciossani, A. Mattevi, O. A. Botrugno, P. Dessanti, *Medchemcomm* **2015**, *6*, 665–670.
- [13] P. Vianello, O. A. Botrugno, A. Cappa, R. Dal Zuffo, P. Dessanti, A. Mai, B. Marrocco, A. Mattevi, G. Meroni, S. Minucci, *J. Med. Chem.* **2016**, *59*, 1501–1517.
- [14] R. Fioravanti, A. Romanelli, N. Mautone, E. Di Bello, A. Rovere, D. Corinti, C. Zwergel, S. Valente, D. Rotili, O. A. Botrugno, et al., *ChemMedChem* **2020**, *15*, 643–658.
- [15] D. Ogasawara, T. Suzuki, K. Mino, R. Ueda, M. N. A. Khan, T. Matsubara, K. Koseki, M. Hasegawa, R. Sasaki, H. Nakagawa, *Bioorg. Med. Chem.* **2011**, *19*, 3702–3708.
- [16] S. Matsuda, R. Baba, H. Oki, S. Morimoto, M. Toyofuku, S. Igaki, Y. Kamada, S. Iwasaki, K. Matsumiya, R. Hibino, et al., *Neuropsychopharmacology* **2019**, *44*, 1505–1512.
- [17] N. Tomita, D. Tomita, Y. Tominari, S. Imamura, S. Morimoto, T. Kojima, M. Toyofuku, Y. Hattori, T. Kaku, M. Ito, WO patent **2014**, 058071.
- [18] L. Liang, H. Wang, Y. Du, B. Luo, N. Meng, M. Cen, P. Huang, A. Ganesan, S. Wen, *Bioorg. Chem.* **2020**, *99*, 103808.
- [19] H. Benelkebir, C. Hodgkinson, P. J. Duriez, A. L. Hayden, R. A. Bulleid, S. J. Crabb, G. Packham, A. Ganesan, *Bioorg. Med. Chem.* **2011**, *19*, 3709–3716.
- [20] Z. Feng, Y. Yao, C. Zhou, F. Chen, F. Wu, L. Wei, W. Liu, S. Dong, M. Redell, Q. Mo, et al., *J. Hematol. Oncol.* **2016**, *9*, 24.
- [21] J. T. Lynch, M. J. Cockerill, J. R. Hitchin, D. H. Wiseman, T. C. P. Somervaille, *Anal. Biochem.* **2013**, *442*, 104–106.
- [22] V. C. Carneiro, I. C. de A. da Silva, M. S. Amaral, A. S. A. Pereira, G. O. Silveira, D. da S. Pires, S. Verjovski-Almeida, F. J. Dekker, D. Rotili, A. Maiid, et al., *PLoS Negl. Trop. Dis.* **2020**, *14*, 1–29.
